

EUROPEAN ORGANIZATION FOR NUCLEAR RESEARCH  
Proposal to the ISOLDE and Neutron Time-of-Flight Committee

**In-source laser spectroscopy of mercury isotopes**

October 10, 2014

L. P. Gaffney<sup>1</sup>, T. Day Goodacre<sup>2,3</sup>, A. N. Andreyev<sup>4</sup>, M. Seliverstov<sup>5,2</sup>, N. Althubiti<sup>3</sup>, B. Andel<sup>11</sup>, S. Antalic<sup>11</sup>, D. Atanasov<sup>10</sup>, A. E. Barzakh<sup>5</sup>, K. Blaum<sup>10</sup>, J. Billowes<sup>3</sup>, T. E. Cocolios<sup>3</sup>, J. Cubiss<sup>4</sup>, G. Farooq-Smith<sup>3</sup>, D. V. Fedorov<sup>5</sup>, V. N. Fedosseev<sup>2</sup>, R. Ferrer<sup>1</sup>, K. T. Flanagan<sup>3</sup>, L. Ghys<sup>1,12</sup>, C. Granados<sup>1</sup>, A. Gottberg<sup>2</sup>, F. Herfurth<sup>8</sup>, M. Huyse<sup>1</sup>, D. G. Jenkins<sup>4</sup>, D. Kisler<sup>10</sup>, S. Kreim<sup>10,2</sup>, T. Kron<sup>7</sup>, Yu. Kudryavtsev<sup>1</sup>, D. Lunney<sup>13</sup>, K. M. Lynch<sup>1,2</sup>, B. A. Marsh<sup>2</sup>, V. Manea<sup>10</sup>, T. M. Mendonca<sup>2</sup>, P. L. Molkanov<sup>5</sup>, D. Neidherr<sup>8</sup>, R. Raabe<sup>1</sup>, J. P. Ramos<sup>2</sup>, S. Raeder<sup>1</sup>, E. Rapisarda<sup>2</sup>, M. Rosenbusch<sup>9</sup>, R. E. Rossel<sup>2,7</sup>, S. Rothe<sup>2</sup>, L. Schweikhard<sup>9</sup>, S. Sels<sup>1</sup>, T. Stora<sup>2</sup>, I. Tsekhanovich<sup>6</sup>, C. Van Beveren<sup>1</sup>, P. Van Duppen<sup>1</sup>, M. Veinhard<sup>2</sup>, R. Wadsworth<sup>4</sup>, A. Welker<sup>14</sup>, F. Wienholtz<sup>9</sup>, K. Wendt<sup>7</sup>, G. L. Wilson<sup>4</sup>, S. Witkins<sup>3</sup>, R. Wolf<sup>10</sup>, K. Zuber<sup>14</sup>

<sup>1</sup>*KU Leuven, Belgium*; <sup>2</sup>*CERN-ISOLDE, CH*; <sup>3</sup>*The University of Manchester, UK*; <sup>4</sup>*The University of York, UK*; <sup>5</sup>*PNPI, Gatchina, Russia*; <sup>6</sup>*CENBG, Bordeaux, France*; <sup>7</sup>*Johannes Gutenberg University of Mainz, Germany*; <sup>8</sup>*GSI, Darmstadt, Germany*; <sup>9</sup>*Ernst-Moritz-Arndt Universität Greifswald, Germany*; <sup>10</sup>*Max-Planck-Institut für Kernphysik, Heidelberg, Germany*; <sup>11</sup>*Comenius University, Bratislava, Slovakia*; <sup>12</sup>*SCK•CEN, Mol, Belgium*; <sup>13</sup>*CSNSM-IN2P3-CNRS, Orsay, France*; <sup>14</sup>*Technische Universität Dresden, Germany*;

**Spokespersons:** Liam Paul Gaffney [[Liam.Gaffney@fys.kuleuven.be](mailto:Liam.Gaffney@fys.kuleuven.be)],  
Thomas Day Goodacre [[Thomas.Day.Goodacre@cern.ch](mailto:Thomas.Day.Goodacre@cern.ch)],  
Andrei Andreyev [[Andrei.Andreyev@york.ac.uk](mailto:Andrei.Andreyev@york.ac.uk)],  
Maxim Seliverstov [[Maxim.Seliverstov@cern.ch](mailto:Maxim.Seliverstov@cern.ch)]  
**Contact person:** Bruce Marsh [[Bruce.Marsh@cern.ch](mailto:Bruce.Marsh@cern.ch)]

**Abstract:** This proposal follows on from the Letter of Intent, I153. The neutron-deficient mercury isotopes are one of the prime examples of shape coexistence anywhere in the nuclear chart. Wide-ranging and complementary experimental and theoretical approaches have been used to investigate their structure over the last few years, however mean-square charge radii are unknown for isotopes with  $A < 181$ . It is proposed to measure the isotope shift (IS) and hyperfine structure (HFS) of the 253-nm transition in  $^{177-182}\text{Hg}$  in an attempt to study the propagation of the famous odd-even staggering behaviour. At the other end of the chain, no information exists on the optical spectroscopy of Hg isotopes beyond the  $N = 126$  shell closure. There is a well-known “kink” in mean-square charge radii beyond this point in the even  $Z \geq 82$  elements. It is proposed to measure the IS of  $^{207,208}\text{Hg}$  in order to provide the first information on this effect below  $Z = 82$ .

**Requested shifts:** 16 shifts, (in a single run)



# 1 Introduction and physics case

Nuclei in the neutron-deficient lead region are famed for their manifestation of shape coexistence [1]. The most striking early evidence came from ISOLDE, with the discovery of a large jump in the mean-squared charge radius between  $^{187}\text{Hg}$  and  $^{185}\text{Hg}$  in isotope shift measurements [2]. This was interpreted as a dramatic change in shape from a weakly-deformed oblate shape in the heavier isotopes to a more-strongly deformed prolate shape in calculations based upon the Strutinsky shell-correction method [3]. Another striking example of shape coexistence occurs in  $^{186}\text{Pb}$ , where the ground state and the first-two excited states are interpreted as the  $0^+$  band heads of three differently-shaped configurations: spherical, oblate and prolate [4]. In the case of the Pb isotopic chain, the isotope shifts [5, 6] indicate that the ground state remains spherical, whereas the Hg isotopes [7] exhibit a more interesting odd-even staggering around the neutron mid-shell (see Fig. 1). This is due to the deformed intruder structure lowering in energy around the neutron mid-shell where it becomes the  $I = 1/2$  ground state in the odd-mass isotopes. The less-deformed structure remains and is apparent in the isomer ( $I = 13/2$ ) shift of  $^{185}\text{Hg}$  and the ground states of the even-even isotopes. In recent years, the improvements of the in-source laser spectroscopy methods using the RILIS at ISOLDE have enabled the determination of mean-square charge radii for some of the most-exotic isotopes in the lead region [8].

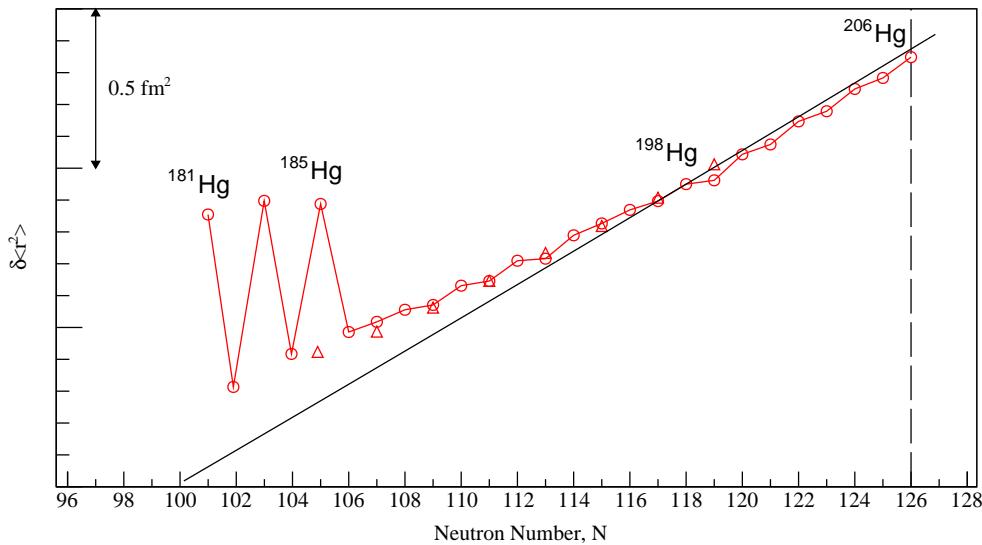


Figure 1: Relative changes in mean-square charge radii for the Hg isotopic chain. The solid line shows the liquid-drop prediction, normalised to  $^{198}\text{Hg}$ . Ground states are represented by circles and isomeric states by triangles. Data taken from Ref. [7].

The neutron-deficient mercury isotopes have recently become a hotbed of experimental activity, with decay [9] and in-beam spectroscopy [10] plus lifetime measurements [11, 12] and Coulomb excitation [13] providing critical information on the nature of excited states. In view of ground-state properties however, the isotope shifts have been measured down to only  $A = 181$  ( $N = 101$ ) [7]. It is expected that the weakly-deformed structure will return to the ground state of the odd-mass isotopes beyond the mid-shell region, as hinted at by in-beam studies of  $^{176,178}\text{Hg}$  [14], but it is yet to be determined at which point it occurs. This collaboration recently investigated similar behaviour in neighbouring  $^{79}\text{Au}$  isotopes (IS534).

At the other end of the Hg isotopic chain, no data on the isotope shift exists beyond the  $N = 126$  shell closure. For all of the heavier elements measured (i.e. Pb, Po, Rn and Ra), a kink, whose underlying mechanism is the source of extensive research and debate [see 15, and references therein], is observed beyond  $N = 126$  (see Figure 3 in Ref [16]). Extending these studies to the neutron-rich isotopes,  $^{207,208}\text{Hg}$ , would provide the first such data in even- $Z$  nuclei below  $Z = 82$ . Complementary  $\beta$ -decay studies with these beams, addressing the structure of excited states, are already underway at ISOLDE (IS588).

## 2 Experimental details

### 2.1 The new RILIS scheme for mercury

Due to pump laser restrictions, the previous RILIS mercury ionisation scheme was based on a reported autoionising state, reachable using the fundamental beam from the frequency-doubled laser providing the second step. The measured efficiency of this scheme was 0.1%, RILIS scheme development to achieve an order of magnitude increase in efficiency was requested by I153 in order for in-source spectroscopy of mercury to be feasible.

The addition of a solid-state pump laser and a complementary Ti:Sa laser system to RILIS brought the possibility of independent second and third excitation steps, enabling a comprehensive scheme development program to be undertaken. Three dye ranges were scanned from three alternative second steps, however, none of the reported autoionising states were seen. It would appear that what was previously thought to be the edge of an autoionising state, was in fact just non-resonant ionisation. A series of Rydberg resonances was observed by scanning a Ti:Sa laser in the vicinity of atomic ionisation threshold and ionisation with a non-resonant final step at 532 nm was also tested using the new RILIS Blaze laser, acquired specifically for the role. Due to the higher power in the ion source, ionisation with this laser was four times more efficient than using the Ti:Sa laser at the best Rydberg resonance. Using the laser ionisation scheme of Figure 2, a laser ionisation efficiency of 6% was measured, meeting the requirements of I153.

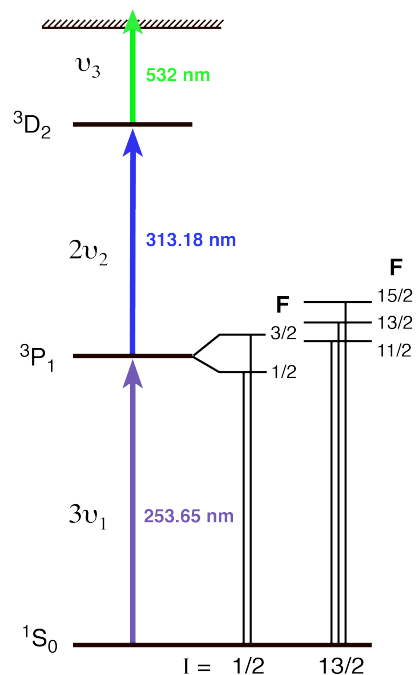


Figure 2: The new RILIS laser ionisation scheme for mercury and the HFS expected to be resolved.

### 2.2 In-source laser spectroscopy

The RILIS setup has been used successfully to measure isotope shifts and HFS in Po down to  $N = 107$  [16–18], Pb down to  $N = 100$  [5, 6] and also long chains of Au, Tl and At isotopes. A new RILIS set-up including improved data acquisition, scanning automation, wavelength stabilisation and continuous laser power monitoring was successfully demonstrated during the latest IS534 run on in-source spectroscopy of astatine isotopes. Through the new RILIS mercury scheme, it is now viable to perform in-source spectroscopy on the

253.7-nm  $6s^2\ ^1S_0 \rightarrow 6s6p\ ^3P_1$  transition with a RILIS Ti:Sa in narrow-band mode, which has a line width (FWHM) of  $\approx 1.5$  GHz after frequency tripling.

At the high temperature conditions of the RILIS cavity, the resolution is limited by the Doppler broadened width, which becomes comparable with the laser linewidth for heavier elements such as mercury. Using the new ionisation scheme, the HFS of  $^{185}\text{Hg}$  was measured during the recent TISD runs, the results are shown in Figure 3.

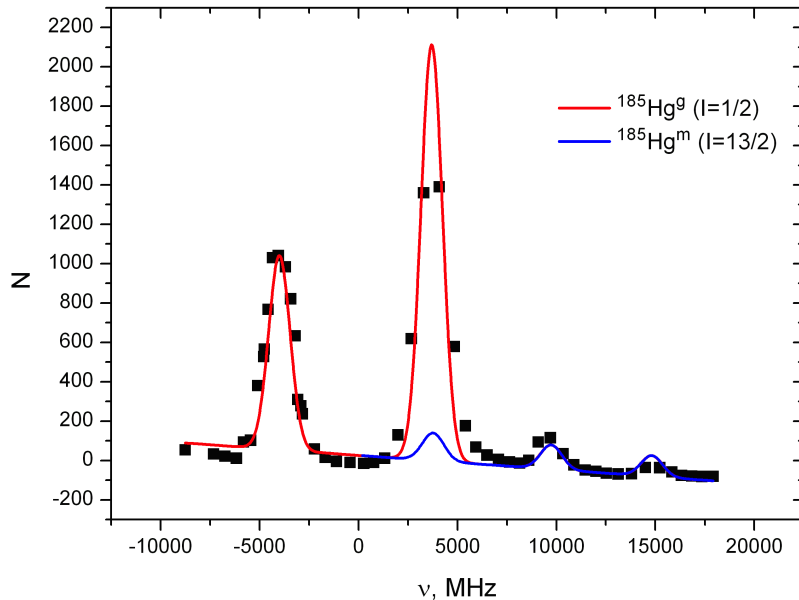


Figure 3: HFS spectrum of  $^{185g,m}\text{Hg}$  measured on a Faraday cup during the I153 tests (24<sup>th</sup> August 2014). The x-axis corresponds to the fundamental frequency of the laser before tripling.

The feasibility of in-source spectroscopy of mercury with the new RILIS scheme and setup is demonstrated by the HFS spectra of Figure 3. The HFS of the ground and the isomeric states can be resolved and fit well with simulations using literature values. This is also a demonstration of the possibility of isomer selective ionisation of  $^{185}\text{Hg}$  using the RILIS lasers.

## 2.3 Ion source development

The original scope of I153 included a comparison of the yields from a molten Pb target [19] coupled with a VADIS FEBIAD-type ion source, as the coupling of a laser/surface ion source hot cavity with a liquid target has yet to be demonstrated, with the yields from a  $\text{UC}_x$  target coupled with a standard laser ion source. Further target development would then have been necessary should the molten Pb target have been required. An alternative approach, which avoids this aspect of target and ion source development, is to couple the RILIS technique with the VADIS cavity. This is shown schematically in Figure 4. Recent off-line tests of laser ionisation of gallium inside the VADIS cavity were promising and two new modes of VADIS operation were established. The three possible modes of VADIS operation are:

**VADIS Mode:** (standard operation) anode voltage 100-130V – electron bombardment and thermal ionisation take place.

**RILIS Mode:** laser beams in VADIS cavity, anode voltage 5V – laser resonance ionisation and thermal ionisation take place.

**VADLIS Mode:** lasers in VADIS cavity, anode voltage 100-130V – laser resonance ionisation, electron bombardment ionisation and thermal ionisation take place.

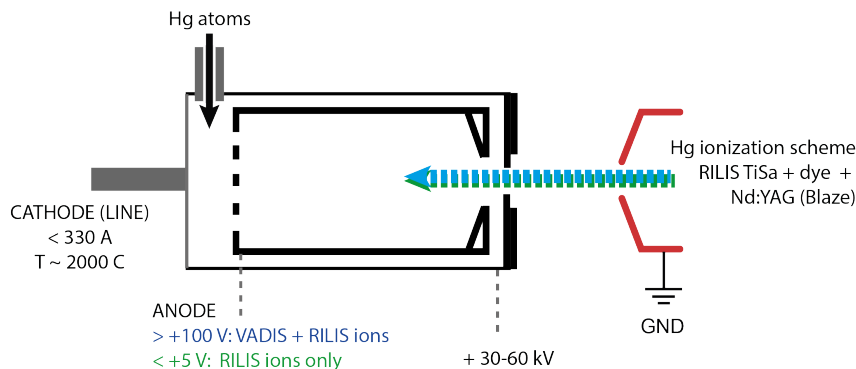


Figure 4: VADIS principles and new operational modes

These new modes were demonstrated online for the first during the I153 tests, some of the results are included in Section 2.4.

## 2.4 Target and production yields

The ion-source developments outlined in Section 2.3 enabled a direct comparison between the molten Pb and the  $\text{UC}_x$  target. With the VADIS operating in standard experimental conditions (cathode heating current 305 A), the RILIS Mode ionisation efficiency for mercury was found to be comparable to when operating in VADIS Mode. Thus, yields measured in VADIS Mode could also be used for expected yields in RILIS Mode. Operation in VADLIS Mode produced a signal nearly equal to the addition of the signals from RILIS Mode and VADIS Mode, with an additional effect believed to be due to the lasers increasing the temperature of the cathode. Operation in VADLIS Mode may be of interest when the requirement is to maximise production, for in-source laser spectroscopy however, it adds an unnecessary background to the laser ionisation signal and would not be employed.

From Figure 5, it can be seen that the  $\text{UC}_x$  target offers comparable yields to the molten Pb, when correcting for the maximum expected proton current ( $0.44\ \mu\text{C}$  for molten Pb and  $1.5\ \mu\text{C}$  for  $\text{UC}_x$ ), at least down to  $^{177}\text{Hg}$  which is the expected lower mass limit of this experiment.  $^{207,208}\text{Hg}$  have recently been seen by IS588 from a molten Pb target using the VADIS in standard VADIS Mode [20]. Their results have been used to calculate the shift requests in Section 3. The use of the newly established RILIS + VADIS combination, as requested in this proposal, would represent the first application of this ion production method for an on-line physics experiment. We should state that the recent the  $\text{UC}_x$  yield measurements were made with a used target with a quartz transfer line. It is believed that, due the volatility of mercury, the diffusion and effusion times would not be significantly influenced.

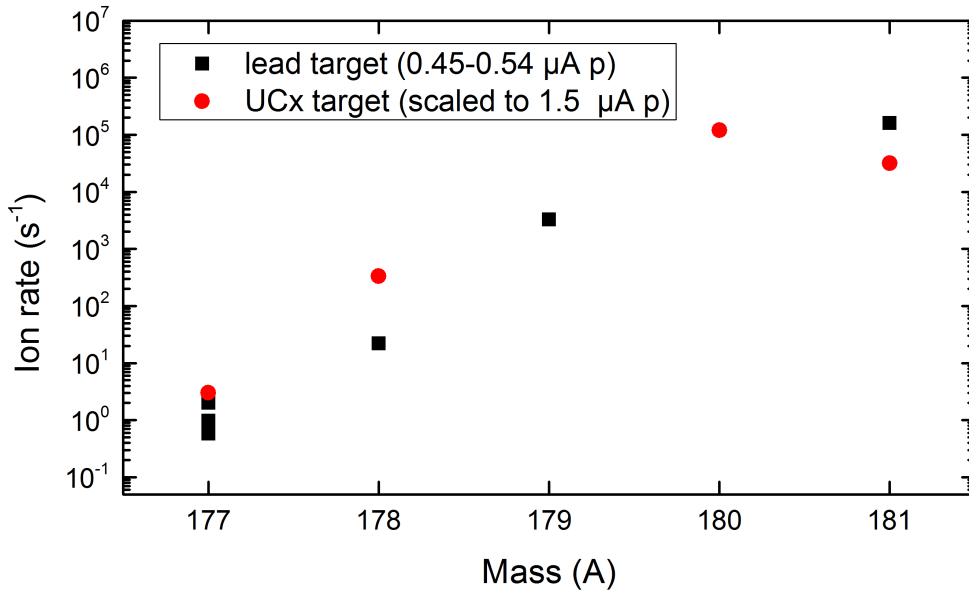


Figure 5: Expected ion rates of the neutron deficient isotopes of interest using laser ionisation. The given rates for the lead target correspond directly with those measured with a proton current between  $0.45 \mu\text{C}$  and  $0.54 \mu\text{C}$ , the  $\text{UC}_x$  values correspond to a linear extrapolation from what was measured to assume a proton current of  $1.5 \mu\text{C}$ .

## 2.5 Windmill set-up

The  $\alpha$ -emitting laser-ionised Hg isotopes will be transmitted to the Windmill (WM) setup, where their decays can be counted at each laser frequency scan position. This technique is described in detail in Ref [18]. The WM consists of a rotating wheel containing 10 thin carbon foils ( $20 \mu\text{g}/\text{cm}^2$ ), onto one of which the incoming beam is deposited. There are Si detectors front and back of the implantation position and again at an off-axis (“decay”) position. The rotation of the wheel is synchronised with the PSB supercycle, meaning that the counting of  $\alpha$  decays can be performed for a fixed period of time, before moving the activity away from the detectors. This rotation also triggers a step change in the laser frequency and hence a scan of 100 steps can be performed in  $\approx 1 - 2$  hours. In addition to the WM system, a HPGe will be placed directly behind the implantation point to gather  $\alpha$ - $\gamma$  coincidences. As a by-product of these measurements, detailed and precision decay spectroscopy can be performed with this setup, similarly to the Po  $\alpha$ -decay and Tl  $\beta$ -decay [9], as well as potential  $\beta$ -delayed fission studies [21]. A study of the possible  $\beta$ -delayed proton emission in  $^{179,181,183}\text{Hg}$  [22] adds additional motivation to these measurements.

## 2.6 Multi-Reflection Time-of-Flight Mass Spectrometer of ISOLTRAP

For the  $\beta$ -emitting neutron-rich isotopes, it is not possible to use the WM setup and the long-lived nature of  $^{208}\text{Hg}$  means that, in this case at least,  $\beta$ -counting at the ISOLDE Decay Station (IDS) is not a possibility either. The Multi-Reflection Time-of-Flight Mass Spectrometer (MR-ToF MS) of the ISOLTRAP experiment [23] was already successfully applied for HFS scanning in long chains of Au and At isotopes (IS534). We expect that mass separation of Hg and Pb isotopes is reliable given that the surface-ionisation of Pb

while in RILIS Mode is expected to be orders of magnitude less efficient than the VADIS ionisation of Pb contaminants seen in IS588 while in VADIS Mode. In order to offer the cleanest possible selection of  $^{207,208}\text{Hg}$ , 1 shift should be dedicated to the selection of the optimal operating parameters for the MR-ToF MS. While scanning  $^{207}\text{Hg}$ , we will also be able to measure the ground-state mass, allowing for a direct comparison with the recently-measured data at ESR@GSI [24]. Furthermore, a simultaneous search for a possible isomeric state will be undertaken. Both these tasks require no additional measurement time.

### 3 Beam-time request

We propose to measure the isotope shift (IS) of the 253.7-nm transition in the even-even mercury isotopes,  $^{178,180,182}\text{Hg}$ , with respect to  $^{198}\text{Hg}$ . Further to this, the isotope/isomer shift of the same transition in the odd-mass isotopes,  $^{177,179,181}\text{Hg}$ , will be measured along with their HFS. For the neutron-rich isotopes with  $N > 126$ , we propose to measure the IS of the same transition in  $^{207,208}\text{Hg}$ . The yield comparison presented in this proposal indicates that molten Pb and  $\text{UC}_x$  targets are comparable in their suitability for the study of neutron deficient mercury down to  $^{177}\text{Hg}$ . The molten Pb target would be preferred however, as it would also enable the measurement of  $^{207,208}\text{Hg}$  to be performed, since it would avoid the problem of the overwhelming background of isobaric Fr that would be extracted from the  $\text{UC}_x$  target. We would request the experiment takes place at GPS, where a transport efficiency of 95% is assumed.

Table 1: Recently measured  $\alpha$ -decay rates from I153 and deduced ISOLDE production yields for Hg isotopes from a molten Pb target. The  $\alpha$ -decay branching ratios,  $b_\alpha$ , are given, the transport efficiency was assumed to be 100% and the  $\alpha$  detection efficiency was 10%. The required measurement times for the proposed experiment are also included.

$A$	$T_{1/2}$ [s]	$b_\alpha$ [%]	$\alpha$ rate [Hz]	$p^+$ [ $\mu\text{A}$ ]	ISOLDE Yield [ions/ $\mu\text{C}$ ]	Req. time [hours]	[shifts]
181	3.6	27	$5.2 \times 10^3$	0.50	$3.3 \times 10^5$	4	} 6 (WM)
179	1.05	55	$1.7 \times 10^2$	0.50	$6.0 \times 10^3$	10	
177	0.1273	85	$1.7 \times 10^{-1}$	0.54	$2.0 \times 10^0$	34	
182	10.83	15.2	$9.0 \times 10^2$	0.09	$6.7 \times 10^5$	7	} 3 (WM)
180	2.58	48	–	–	$(2.0 \times 10^4)^\dagger$	7	
178	0.2665	70	$4.5 \times 10^0$	0.38	$1.7 \times 10^2$	10	
207	174	pure $\beta$			$(\approx 10^6)^*$	8	} 3 (MR-ToF)
208	2460	pure $\beta$			$(\approx 10^2)^*$	16	

<sup>†</sup>extrapolated; \*estimated from IS588 experiment with VADIS. RILIS ionisation is expected to be lower

It has been demonstrated in the past that laser spectroscopy can be performed on even-even nuclei with production rates lower than 1 ion per second [16]. In the cases presented here with low production yields, specifically  $^{177,208}\text{Hg}$ , scan times can be increased to collect sufficient statistics (a minimum of 50 events ( $\alpha$ -decays or ions) detected on resonance to ensure reliable fitting of the spectra). For  $^{181}\text{Hg}$ , where the isotope shift has already been measured, we require two frequency scans, one in each direction, for a HFS measurement to

test our method for systematic error. In  $^{177,179,207}\text{Hg}$ , the isotope shift and HFS is unknown and therefore we request a minimum of four scans per isotope. In the even-mass isotopes, where only one peak is expected in the HFS spectrum, we require three scans each to measure the isotope shift. The required measuring time in Table 1 does not include the time taken to change measurement settings from one isotope to another, i.e. mass settings of the separator and laser frequency. In addition, at least one scan of the reference isotope will be required every shift to ensure the stability of the system. This time is counted separately and amounts to 16 hours (2 shifts) in total. If running on HRS, as opposed to the preferred GPS, the transmission is expected to be reduced significantly. This, in addition to the longer time required to change mass, which is to be done for every reference measurement and isotope change, will necessitate a longer running time.

**Summary of requested shifts:** In total, we are requesting **16 shifts**. This breaks down as **9 shifts** to measure the IS of the 253-nm transition for the first time in the neutron-deficient  $^{177-180,182}\text{Hg}$  and simultaneously perform HFS spectroscopy on the odd-mass isotopes. Within this,  $^{181}\text{Hg}$  will also be remeasured, to compare to literature values and test any systematic uncertainties in our method. **3 shifts** are requested to measure the IS of the same transition in the neutron-rich  $^{207,208}\text{Hg}$  for the first time. **2 shifts** are also required for the regular measurements of the reference isotope,  $^{198}\text{Hg}$ . **1 shift** is required for the setup and optimisation of RILIS, and a further **1 shift** for MR-ToF. In parallel, wide-ranging decay spectroscopy will be performed in the  $n$ -deficient isotopes, requiring 0 additional shifts.

## References

- [1] K. Heyde and J. L. Wood, *Rev. Mod. Phys.* **83**, 1467 (2011).
- [2] J. Bonn, G. Huber, H.-J. Kluge, L. Kugler, and E. Otten, *Phys. Lett. B* **38**, 308 (1972).
- [3] S. Frauendorf and V. Pashkevich, *Phys. Lett. B* **55**, 365 (1975).
- [4] A. N. Andreyev et al., *Nature* **405**, 430 (2000).
- [5] H. De Witte et al., *Phys. Rev. Lett.* **98**, 112502 (2007).
- [6] M. D. Seliverstov et al., *Eur. Phys. J. A* **41**, 315 (2009).
- [7] G. Ulm et al., *Zeitschrift für Phys. A At. Nucl.* **325**, 247 (1986).
- [8] V. N. Fedosseev, Y. Kudryavtsev, and V. I. Mishin, *Phys. Scr.* **85**, 058104 (2012).
- [9] J. Elseviers et al., *Phys. Rev. C* **84**, 034307 (2011).
- [10] M. Scheck et al., *Phys. Rev. C* **83**, 037303 (2011).
- [11] T. Grahn et al., *Phys. Rev. C* **80**, 014324 (2009).
- [12] L. P. Gaffney et al., *Phys. Rev. C* **89**, 024307 (2014).
- [13] N. Bree et al., *Phys. Rev. Lett.* **112**, 162701 (2014).
- [14] R. Julin, K. Helariutta, and M. Muikku, *J. Phys. G Nucl. Part. Phys.* **27**, R109 (2001).
- [15] P. Goddard, P. Stevenson, and A. Rios, *Phys. Rev. Lett.* **110**, 032503 (2013).
- [16] T. E. Cocolios et al., *Phys. Rev. Lett.* **106**, 052503 (2011).
- [17] M. Seliverstov et al., *Phys. Lett. B* **719**, 362 (2013).
- [18] M. D. Seliverstov et al., *Phys. Rev. C* **89**, 034323 (2014).
- [19] J. Lettry et al., *Nucl. Instrum. Meth. Phys. Res. Sect. B* **126**, 170 (1997).
- [20] Podolyak, Z., Private Communication [z.podolyak@surrey.ac.uk](mailto:z.podolyak@surrey.ac.uk).
- [21] A. N. Andreyev et al., *Phys. Rev. Lett.* **105**, 252502 (2010).
- [22] P. Hornshøj et al., *Phys. Lett. B* **34**, 591 (1971).
- [23] R. Wolf et al., *Int. J. Mass Spectrom.* **349-350**, 123 (2013).
- [24] L. Chen et al., *Nucl. Phys. A* **882**, 71 (2012).

# Appendix

## DESCRIPTION OF THE PROPOSED EXPERIMENT

The experimental setup comprises a Windmill system with 2-4 Si detectors inside, and 1-2 Ge detectors outside. WM system was successfully used in the runs IS387, IS407, IS456, IS466, I-086 and IS534, therefore solid understanding of all possible hazards is available.

Part of the	Availability	Design and manufacturing
Windmill	<input checked="" type="checkbox"/> Existing	<input checked="" type="checkbox"/> To be used without any modification
ISOLTRAP + MR-ToF MS	<input checked="" type="checkbox"/> Existing	<input checked="" type="checkbox"/> To be used without any modification

HAZARDS GENERATED BY THE EXPERIMENT: Hazards named in the document relevant for the fixed ISOLTRAP + MR-ToF MS installation.

Additional hazards:

Hazards	Windmill	ISOLTRAP + MR-ToF MS
<b>Thermodynamic and fluidic</b>		
Pressure	–	
Vacuum	Standard ISOLDE vacuum	
Temperature	–	
Heat transfer	–	
Thermal properties of materials		
Cryogenic fluid	LN <sub>2</sub> , 2 Bar, 150 l	
<b>Electrical and electromagnetic</b>		
Electricity	Standard power supplies	
Static electricity	–	
Magnetic field	–	
Batteries	<input type="checkbox"/>	
Capacitors	<input type="checkbox"/>	
<b>Ionizing radiation</b>		
Target material [C foils]	The C foils, where the radioactive samples are implanted, are very fragile. Should they break upon opening the Windmill, the pieces are so light that they would become airborne. Great care must be taken when opening the system and removing them (slow pumping/venting protective equipment: facial mask).	
Beam particle type (e, p, ions, etc)		
Beam intensity		

Beam energy		
Cooling liquids	[liquid]	
Gases	[gas]	
Calibration sources:	<input type="checkbox"/>	
• Open source	<input type="checkbox"/>	
• Sealed source	<input type="checkbox"/> [ISO standard]	
• Isotope	$^{239}\text{Pu}$ , $^{241}\text{Am}$ , $^{244}\text{Cm}$	
• Activity	1 kBq each	
Use of activated material:		
• Description	<input type="checkbox"/>	
• Dose rate on contact and in 10 cm distance	[dose][mSV]	
• Isotope		
• Activity		
<b>Non-ionizing radiation</b>		
Laser	Standard RILIS operation	
UV light		
Microwaves (300MHz-30 GHz)		
Radiofrequency (1-300 MHz)		
<b>Chemical</b>		
Toxic	Pb shielding, 30-40 bricks	
Harmful	–	
CMR (carcinogens, mutagens and substances toxic to reproduction)	[chem. agent], [quant.]	
Corrosive	–	
Irritant	–	
Flammable	–	
Oxidizing	–	
Explosiveness	–	
Asphyxiant	–	
Dangerous for the environment	–	
<b>Mechanical</b>		
Physical impact or mechanical energy (moving parts)	The chamber is heavy and needs to be handled with care during installation/ removing.	
Mechanical properties (Sharp, rough, slippery)	–	
Vibration	–	
Vehicles and Means of Transport	–	

<b>Noise</b>		
Frequency	–	
Intensity	–	
<b>Physical</b>		
Confined spaces	–	
High workplaces	–	
Access to high workplaces	–	
Obstructions in passageways	–	
Manual handling	–	
Poor ergonomics	–	

Hazard identification:

Average electrical power requirements (excluding fixed ISOLDE-installation mentioned above): Negligible